

Available online at www.sciencedirect.com**ScienceDirect**

Energy Procedia 85 (2016) 481 – 488

Energy

Procedia

Sustainable Solutions for Energy and Environment, EENVIRO - YRC 2015, 18-20 November
2015, Bucharest, Romania

CFD study on convective heat exchange between impinging gas jets and solid surfaces

Ștefan-Mugur Simionescu^{a*}, Corneliu Bălan^a

^aREOROM Group, Hydraulics Department, University "Politehnica" of Bucharest, 313 Splaiul Independentei sector 6,
060042 Bucharest, Romania

Abstract

The paper is concerned with a CFD numerical investigation using the Fluent code of the convective heat exchange between an impinging gas jet at room temperature and a structured solid surface with square-shaped grooves which is maintained at constant temperature of 80°C. Reynolds averaged Navier-Stokes simulations coupled with the energy equation are performed for a planar jet on a 3D domain with periodic boundary conditions.

The range of jet Reynolds numbers used for the simulations is in the interval from 2000 to 10000, while the jet standoff distance can take different values, ranging from 2 to 10 times the jet width $b=2$ mm. The detailed distribution of the convective heat transfer coefficient and the mean Nusselt number at the impingement of the air jet on the impacted plate will be inferred. Finally, a comparison between the numerical results, a set of experiments performed and relevant cases from literature is made and conclusions are drawn. One main result of the study is the confirmation of the numerical procedure for the domain used.

© 2016 The Authors. Published by Elsevier Ltd. This is an open access article under the CC BY-NC-ND license

(<http://creativecommons.org/licenses/by-nc-nd/4.0/>).

Peer-review under responsibility of the organizing committee EENVIRO 2015

Keywords: Heat transfer coefficient; Nusselt number; structured surface; CFD simulation

1. Introduction

Due to their industrial importance, impinging jet flows have received considerable attention, with particular interest in the modification of heat transfer at the wall. In practical applications, impinging jets are efficient tools in cooling or heating systems through their ability to enhance heat transfer between the fluid and the impinged solid target. In particular, the use of structured surfaces allows a further growth of the heat transfer, due to an increased

* Corresponding author. Tel.: +4-074.390.5552; Fax: +4-021.318.1015.

E-mail address: stefan_simionescu@yahoo.com

fluid-solid interface area. The cooling of aircraft engines is an example where impinging jets are used to enhance the heat transfer [1]. Another example where structured surfaces are used in the cooling of electronic equipment is presented in references [2] and [3].

The near-wall vortical structures of impinging jet flow have been extensively investigated experimentally – some comprehensive reviews were found in [4], others in [5] and [6]. Some of the first impinging jet flow experiments are summarized in the review of Gauntner, Livingood & Hrycak [7]. These experiments are mainly focused on basic turbulent statistics allowing the identification of characteristic flow regions and regimes.

The impinging jet flow is commonly divided into three regions [1]: first, the free jet region is defined as the region where the flow is not influenced by the impingement plate. In this zone, the velocity is mainly axial and constant on the jet centerline. Second, in the stagnation region, the flow is deflected from its axial direction to a radial one. Third, in the wall jet region, the velocity is mainly radial, with the formation of a boundary layer developing along the radial direction. The boundary layer velocity profile is shaped as for a wall jet flow, with a maximum velocity at an intermediate distance from the wall. With increasing radial distance, its thickness increases whereas its maximum velocity decreases.

Forced convection is a mechanism of heat transfer in which the fluid motion is generated by an external source. This type of heat transport can be found in everyday life like air conditioning, central heating and many other mechanisms [8]. The *Reynolds number* and the distance from the jet exit to the wall are playing a significant role.

Numerical simulations using RANS models and flat impinging surfaces have been widely used to predict different kinds of turbulent flows, primary due to their simplicity and reduced computational costs. Such a study was published by Heyerichs and Pollard [9], who examined an impinging slot jet at a Reynolds number of 10,000. Wang and Mujumdar [10] compared five low Reynolds RANS models for the Reynolds numbers 5200 and 10,400 and two dimensionless jet-to-surface spacings of 2.6 and 6.

The main objective of this article is to study the influence of a specific configuration of structured surface on a jet, on the heat transfer point of view, by using the numerical approach. The design of the surface may influence the jet development and consequently may affect the convective heat transfer. The impinging jet is formed by using a slot nozzle.

2. Theoretical aspects

2.1. Impinging jets

When a wall is interposed in a free jet, a new pattern of flow appears due to the jet-wall interaction. The disturbance created by a solid wall on an impinging jet is propagated upstream at a rate equal to the difference between the sonic velocity and the fluid velocity [11]. The wall effect diminishes therefore with increasing Mach number and it finally disappears at Mach number equals one, when the disturbance created by the wall does not anymore propagate upstream.

Theoretical and experimental studies show that no surface effect exists beyond a distance of about two jet diameters from the impinging plate. Consequently, an impinging jet can be considered to behave like a free jet, except in the immediate vicinity of the impingement surface.

A fundamental importance in the study of impinging jets presents the distinction between laminar and turbulent jets. There are many studies on this subject, but sometimes they show different results, so it is not possible to have a general rule about this. A first classification, but not general, based on a critical Reynolds number Re_0 , based on the nozzle diameter and the fluid velocity at the nozzle is given by Gardon [11], which distinguishes laminar from turbulent jets at $Re_0 \cong 1000$. Four characteristic jet patterns for free jets were reported, namely:

- Fully laminar jets, $300 < Re_0 < 1000$. There is no noticeable diffusion of the jet into the surrounding fluid.
- Transition or semi-turbulent jets, $1000 < Re_0 < 3000$
- Fully turbulent jets, $Re_0 > 3000$.

The preceding discussion relating jet flow regimes to Re_0 range dealt only with jets issuing from circular nozzles. However, it applies also to the case of slot jets as Gardon and Akfirat [12] points out that slot jets are becoming

transitional at $650 < Re_0 < 950$ and are turbulent for $Re_0 > 2000$ – here, the Reynolds number Re_0 is based on the nozzle width b .

2.2. Natural and forced convection

Natural convection is a mechanism of heat transfer in which the fluid motion is not generated by external source but only by density differences in the flow due to existence of temperature gradients. In the case of natural convection flow, the heat source produces heat which causes the surrounding air to become less dense and rise. This is the flow formed through buoyancy effect. In the case of forced convection, fluid motion is generated by an external source, in the present case the air jet emerging from the slot nozzle perpendicular to the impingement plate. Figure 2.1 presents sketches of both convection models.

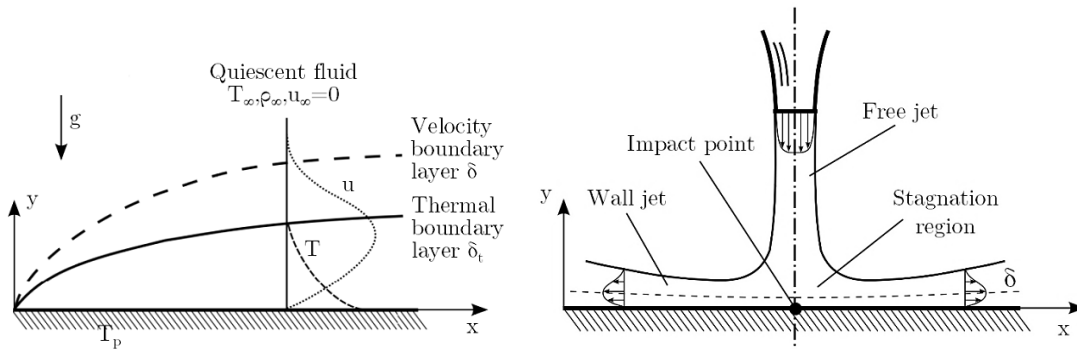


Figure 2.1 Natural (left) and forced (right) convection mechanisms

2.3. Non-dimensional parameters

The first non-dimensional parameter used is the *Reynolds number*, ratio of the inertia and viscous forces [13]:

$$Re = \frac{\rho v L}{\eta} \quad (1)$$

where ρ is the fluid density (kg/m^3), v is the fluid velocity (m/s), L is the characteristic length (m) and η is the dynamic viscosity ($Pa \cdot s$).

The *Nusselt number* which constitutes the ratio of convection to pure conduction heat transfer is defined as [13]:

$$Nu = \frac{hL}{k_f} \quad (2)$$

where h stands for convective heat transfer coefficient of the flow (W/m^2K), L is the characteristic length (m) and k_f is the thermal conductivity of the fluid (W/mK).

The parameter y^+ represents the non-dimensional wall distance for a wall-bounded flow [14]:

$$y^+ = y \frac{u_\tau}{\nu} \quad (3)$$

where y is the distance from the wall (m), u_τ is the friction velocity at the nearest wall (m/s) - a form by which a shear stress can be re-written in units of velocity, and ν is the kinematic viscosity (m^2/s).

Another parameter is z/b , which constitutes the way of nondimensionalizing the distance z between the jet nozzle and the plate by the jet width b .

3. Computational domain and mesh

For the present study case a plate with one-direction equidistant grooves with square section of 4x4 mm is simulated, as presented in Figure 3.1. The slot nozzle is placed perpendicular to the grooves direction.

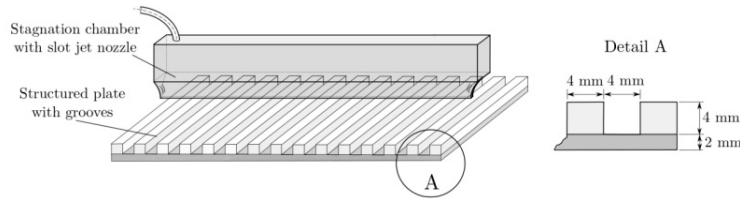


Figure 3.1 Sketch of the structured plate

In order to ensure good numerical results, a special 3D geometry and discretization were realized, by using the Gambit meshing software, reproducing one of the grooves from the structured plate. The periodicity condition was used for the domain to avoid a too high number of mesh elements and a too long computing time. In the same time, a symmetry condition was avoided, to allow a full development of the jet. The domain is presented in Figure 3.2. A single mesh was realized for this case, with 795472 cells. The maximum y^+ value at $Re = 10000$ was computed as 5.

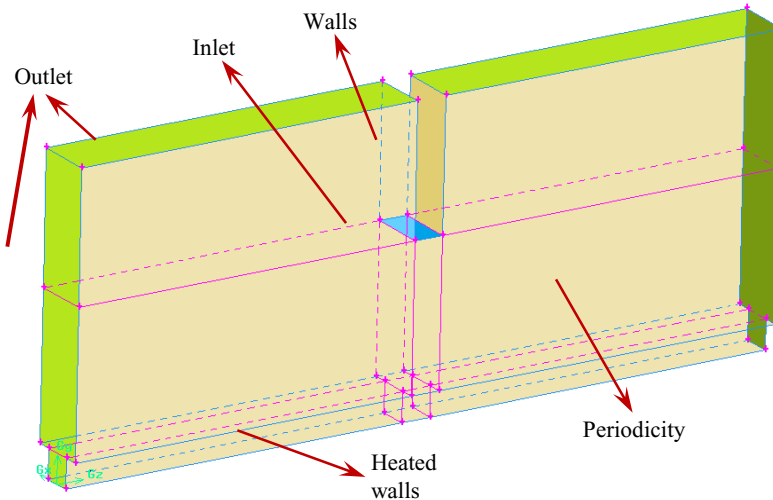


Figure 3.2 Computational domain and boundary conditions

In order to allow meshing in an easier way and in the same time because a structured mesh was desired, the 3D domain was splitted into 8 smaller volumes which were discretized separately. The attention for a more refined mesh was directed to the more sensitive areas at the inlet (the face corresponding to the inlet face has 20x48 mesh cells), sharp edges on the grooves and close to the solid walls. Two details of the mesh are presented in Figure 3.3.

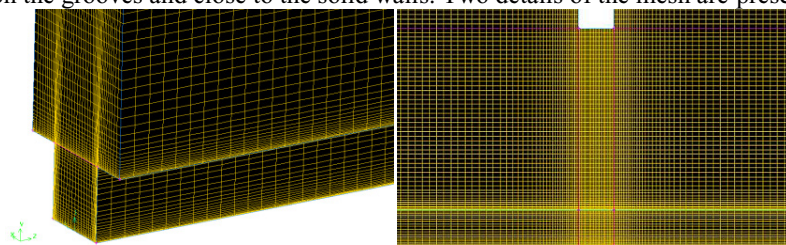


Figure 3.3 Details of mesh: groove zone (left) and inlet area (right)

The geometrical dimensions of the domain defined for computations are dependent on the nozzle width and the nozzle-to-plate distance. The outlet border should be placed at a sufficiently large radial distance, so that error arising from the application of outlet-pressure condition will not significantly affect the region of interest. For the simulations, an unconfined domain was considered. According to the references [1] and [15], the radial expansion of the flow domain was chosen at $15b$. Another consideration is about the vertical distance from the nozzle mouth to the upper boundary of the domain, as from the latter some flow entrainment can occur. Then, a sufficient large distance between them is necessary in order to limit boundary influences. A four nozzle widths distance from the nozzle mouth to the upper boundary was selected.

Some equally important conditions are the profiles of velocity and turbulence at the inlet. For simplifying the test cases, these were kept constant for all the study cases. The velocity was imposed corresponding to the desired Reynolds number, as for the turbulence conditions, a turbulence intensity of 10% and the hydraulic diameter of the jet nozzle were imposed before running the simulations. The no-slip boundary condition was enforced at the solid walls. In addition, for the heated walls a constant temperature of 80°C was imposed as thermal boundary condition.

4. Results

4.1. Turbulence models

A comparison between numerical results given by different turbulence models in terms of Nusselt number distribution, computed for the case with $Re = 10000$ and $z/b = 2$, can be seen in Figure 4.1.

The RANS data achieved within the present study are compared with DNS data obtained from Dairay [1], for the same Reynolds number and jet standoff distance, on a domain with the same boundary conditions but with a circular jet nozzle. Overall, the form of the Nusselt number distribution resulting from the simulation shows a similar magnitude with the one coming from the DNS data. The case that best fits the DNS results is the one given by $k - \omega$ SST turbulence model, which is the reason why it will be used for the numerical test cases throughout the study. The first peak is present at radial position $x/b \approx 0.6$ and has the same Nusselt number value, whereas the second peak, although emerging at $x/b \approx 2$, similar to the DNS results, has a significantly lower magnitude, showing a limit of the RANS models.

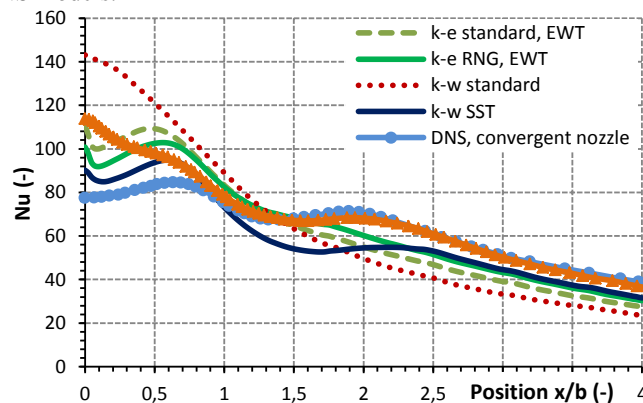


Figure 4.1 Nusselt number distribution for different turbulence models; comparison with DNS results of Dairay [1]

4.2. Velocity field

The velocity pathlines on longitudinal and a transversal central planes with respect to the plate grooves are plotted in Figure 4.2. In the longitudinal plane, the four zones of the impinging jet described in Chapter 1 can be well distinguished. The influence of the groove on the velocity field can be also qualitatively deduced by mean of two contrarotating vortices inside the groove.

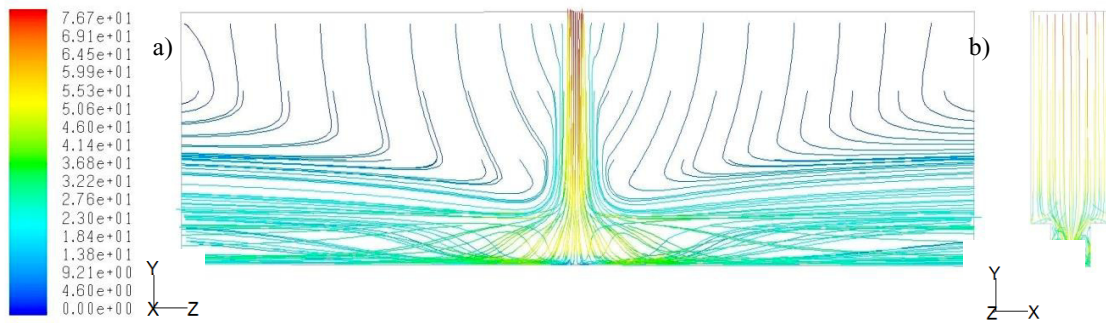


Figure 4.2 Velocity pathlines coloured by velocity magnitude on a longitudinal central plane (a) and transversal central plane (b) with respect to the grooves direction

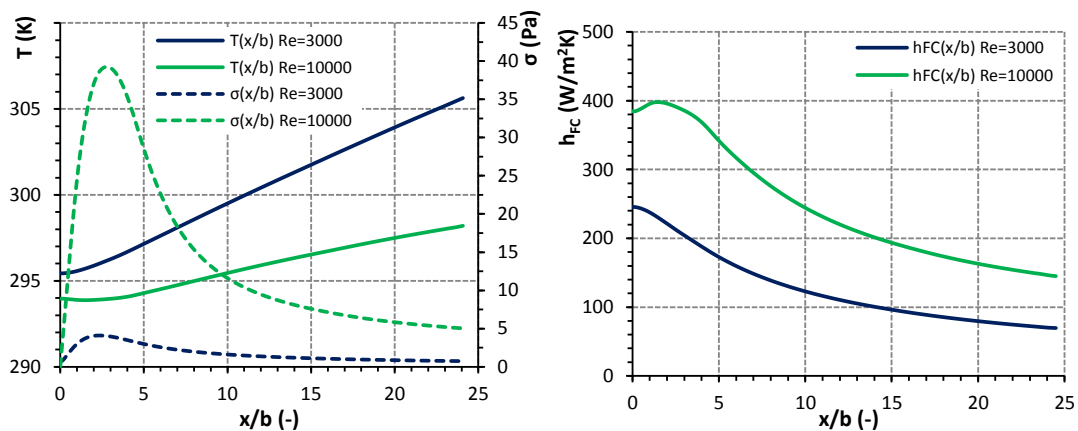


Figure 4.3 Temperature, wall shear stress (a) and heat transfer coefficient distributions (b) for two different Reynolds numbers

4.3. Distributions of wall shear stress, temperature and heat transfer coefficient

A comparison in terms of wall shear stress, temperature and forced convection heat transfer coefficient distributions for two different Reynolds numbers at $z/b = 5$ is presented in Figure 4.3. The shape of the profiles is similar but the magnitude changes with the Reynolds number.

A comparison in terms of forced convection heat transfer coefficient, between the numerical data and a case with the same flow conditions acquired experimentally and presented in reference [16] is presented in Figure 4.4. The two numerical profiles corresponding to the 3D case show a similar shape with the experimental data, yet the overall magnitude of the profiles is different. The reason for this shift is the neglecting of conduction inside the plate, as well as considering the ideal case for the numerical simulation. A more accurate numerical study, taking into account the conduction influence and using conjugated heat transfer would be therefore recommended.

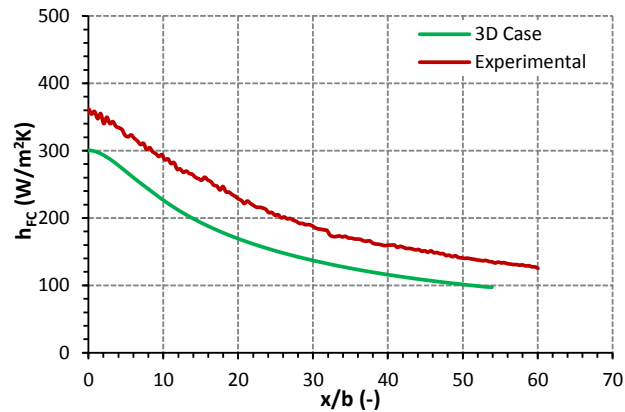


Figure 4.4 Comparison on h_{FC} between numerical and experimental data from [16] for $Re = 5000$ and $z/b=2$

5. Conclusion

The objective of this numerical study was to characterize the convective heat transfer for an impinging jet from a slot nozzle against a structured plate with equidistant square grooves. A set of CFD RANS simulations were performed, on a specially built computational domain: 3D case with periodic boundary condition, which reproduces one groove of the structured plate.

Changes of the Nusselt number, and especially those related with the secondary peak, were checked. Most of the RANS turbulence models were found not to bring a reasonable prediction of the Nusselt number trend. Better results were obtained with the $k - \omega SST$ turbulence model, and in some extent with $k - \varepsilon RNG$. Comparisons were made between the numerical results achieved and data coming from DNS simulations found in the literature and experimental data.

DNS results are today more and more present in the literature for cases related to the studied ones. If good understood and interpreted, they can provide a precious support and even the validation required for the RANS numerical cases.

Imposing a realistic velocity profile at the inlet and a better value for the turbulence intensity are part of our future research plans. A way to predict a better value for the turbulence intensity is to use the formula from [17]. Also, for a fully developed velocity profile, a way is to do the numerical simulation on a larger domain, upstream the slot, so the fluid will have enough distance to evolve a realistic velocity profile. An extension of this work to cases with higher Reynolds numbers may be also attractive, references [3] and [8] point out interesting behaviours for jets with higher level of turbulence.

Acknowledgements

The authors would like to acknowledge the support of the Von Karman Institute for Fluid Dynamics, Rhode Saint- Genese, Belgium, where the study took place.

The work has been funded by the Sectorial Operational Programme Human Resources Development 2007-2013 of the Ministry of European Funds through the Financial Agreement POSDRU/159/1.5/S/132395. The authors acknowledge the financial support from the grants of the Ministry of National Education CNCS-UEFISCDI: PNII-ID-PCE-2012-4-0245.

References

- [1] Dairay T., Fortuné V., Lamballais E., Brizzi L. E. Direct numerical simulation of a turbulent jet impinging on a heated wall. *Journal of Fluid Mechanics*, 2015, Vol. 764, pp. 362-394;
- [2] Anvarullah M., Vasudeva Rao V., Sharma K. V. Effect of nozzle spacing on heat transfer and fluid flow characteristics of an impinging circular jet in cooling of electronic components. *Int. Journal of Thermal & Environmental Engineering* 2012, Volume 4, No. 1, pp. 7-12;
- [3] Wang Z., Mayinger F. Natural convection and heat transfer in the PCB's array of electronic equipments. *Proceedings of the 1st Baltic Heat Transfer Conf.*, Göteborg, Sweden. Aug. 26-28, 1991.
- [4] Jambunathan, K., Lai, E., Moss, M. A., Button, B. L. A review of heat transfer data for single circular jet impingement, *International Journal of Heat and Fluid Flow*, Vol. 13, No. 2, 1992, pp. 106-115;
- [5] Geers, L., Hanjalic, K., Tummers, M. J. Wall imprint of turbulent structures and heat transfer in multiple impinging jet arrays, *Journal of Fluid Mechanics*, vol. 546, 2006, pp. 255–284;
- [6] Benmouhoub, D., Mataoui, A. Turbulent heat transfer from a slot jet impinging on a flat plate, *Journal of Heat Transfer*, Nr. 135 (10), 2013;
- [7] Gauntner, J., Livingood, J., Hrycak, P. Survey of literature on flow characteristics of a single turbulent jet impinging on a flat plate, *NASA Technical Note D-5652*, 1970;
- [8] Buchlin, J.-M. Convective heat transfer in impinging-gas-jet arrangements, *Journal of Applied Fluid Mechanics*, Vol. 4, No. 2, Issue 1, 2011, pp. 137-149;
- [9] Heyerichs, K., Pollard, A. Heat transfer in separated and impinging turbulent flows, *International Journal of Heat and Mass Transfer* 39 (12), 1996, pp. 2385-2400;
- [10] Wang, S. J., Mujumdar, A. S. A comparative study of five low Reynolds number k- ϵ models for impingement heat transfer, *Flow, Turbulence Combust.* 25 (1), 2005, pp. 31-44;
- [11] Gardon, R., Akfirat, J. C. The role of turbulence in determining the heat-transfer characteristics of impinging jets. *International Journal of Heat and Mass Transfer*, vol. 8, 1965, pp. 1261-1272;
- [12] Gardon, R., Akfirat, J. C. Heat transfer characteristics of impinging two-dimensional air jets, *A.S.M.E. Journal of Heat Transfer*, 88, 1966, pp. 101-108;
- [13] Incropera, F. P., DeWitt, D., Bergman, Th., Lavine, A. *Fundamentals of heat and mass transfer*, 5th edition, John Wiley&Sons Inc., 2000;
- [14] Degrez G. Two-dimensional boundary layers, Revised edition, Course note 143, Von Karman Institute for Fluid Dynamics, November 2013;
- [15] Rohlf, W., Haustein, H., Garbrecht, O., Kneer, R. Insights into the local heat transfer of a submerged impinging jet: Influence of local flow acceleration and vortex-wall interaction, *Int. J. of Heat and Mass Transfer* Vol. 55, 2012, pp. 7728-7736;
- [16] Simionescu, Ș.-M. Convective heat exchange between impinging gas jets and structured solid surfaces, Project report 2015-34, Von Karman Institute for Fluid Dynamics, June 2015;
- [17] Jaramillo, J. E., Trias, F. X., Gorobets, A., Perez-Segarra, C. D., Oliva, A. DNS and RANS modelling of a turbulent plane impinging jet, *International Journal of Heat and Mass Transfer*, vol. 55, 2012, pp. 789-801.